Hydrol. Earth Syst. Sci. Discuss., 11, 12627–12657, 2014
www.hydrol-earth-syst-sci-discuss.net/11/12627/2014/
doi:10.5194/hessd-11-12627-2014

Hydrology and Earth System Sciences
Discussions
Open Access

Characterization of sediment layer composition in a shallow lake: from open water zones to reed belt areas

I. Kogelbauer and W. Loiskandl

Institute of Hydraulics and Rural Water Management, University of Natural Resources and Life Sciences, Vienna, Muthgasse 18, 1190 Wien, Austria

Received: 2 October 2014 – Accepted: 27 October 2014 – Published: 13 November 2014

Correspondence to: I. Kogelbauer (ilse.kogelbauer@boku.ac.at)

Published by Copernicus Publications on behalf of the European Geosciences Union.

Abstract

Lake sediment characterization, a pre-requirement for the vulnerability assessment of lake ecosystems, demands reliable in situ methods for the characterization of the sediment layer composition. A unified characterization of lake sediments within different lake ecotopes (open water, open water patches within the reed, and the reed) is still a challenge. Each ecotope is covered by different classical scientific disciplines (hydrography and terrestrial remote sensing to soil physics) with their specific characterization methods. However, a complementary tool that bridges the gap between land- and hydrographic surveying methods is still missing. Therefore a combination of soil physical sensors (a capacitive sensor and a cone penetrometer) in a measuring system (CSPS) was introduced. CSPS is a non-acoustic device for the rapid in situ delineation of water-mud-consolidated lakebed interfaces. The system was successfully applied across the different ecotopes at the Neusiedler See, a well-mixed shallow lake rich in fine-grained sediments. The geo-referenced vertical CSPS profiles show ecotope-specific layer composition. The effect of wind induced turbidity, particle size, and electrical conductivity were analysed. The water–mud interface was precisely delineated at the open water due to a persistent high water content gradient, equivalent to a lutocline. The penetration resistance for open water showed either a shallow and highly-compacted consolidated lakebed or a consolidated lakebed with a partially compacted layer above; while in the reed the penetration resistance smoothly increased until reaching the deepest penetration depths.

1 Introduction

Lake sediment investigations represent a powerful tool for the support of lake risk assessment in view of changing climate conditions and human impacts (Tolotti, 2012). The horizontal lake management suggests that a lake risk assessment should also

HESSD
11, 12627–12657, 2014

comprise the vulnerability of the reed belt and wetlands around the lake (Soja and Soja, 2014).

In view of that, the investigation of the sediment layer composition within the environmentally different ecotopes of a lake requires a reliable in situ method where the same sediment body is investigated from terrestrial and water site. Near-surface geophysical methods are commonly used to provide detailed stratigraphic information of the sediment body by means of high-resolution spatial images. But Missiaen et al. (2008) stated that a blank data spot remains at the land–water transition where the land-based and the marine geophysical techniques do not converge. Thus, the test of different geophysical techniques (marine sub-bottom profiling, seismic reflection measurements, geo-electrical and electromagnetic measurements, cone penetration test, and manual coring) indicated that only an integrated use and no single technique can provide relevant information. The acoustic methods, especially echo sounding, provided the most comprehensive spatial interpretation of sedimentary structure together with the valuable ground-truth information of the penetration test and the coring (Missiaen et al., 2008). Acoustic echo sounding techniques are widely used for spatial scanning of the bed-topography in marine and lake environments, usually in order to ensure the navigability of shipping pathways (McAnally et al., 2007; Schrottke et al., 2006). But in environments rich in fine-grained sediments the interpretation of the sediment structure – especially the delineation of the mud layer – is challenging and requires measurements of sediment properties at appropriate resolution (Lambert et al., 2002; Schettini et al., 2010). Hence, additional measurements are performed with optical or acoustic sensors to derive the suspended solids concentrations (SSC) (McAnally et al., 2007; Schettini et al., 2010; Shi et al., 1996; Teeter, 1992; Wolanski et al., 1989), non-acoustical direct devices such as the cone penetration testing with pore pressure measurement (Seifert and Kopf, 2012; Seifert et al., 2008), or the coring for the ground truth (Lambert et al., 2002). The additional information aims to improve the layer delineation along a continuous vertical profile of sediment properties showing distinctive interfaces of water-mud-consolidated bed sediments. But still those methods were only applied at the open water.

Thus, a combination of soil physical sensors in a measuring system (CSPS) was introduced in Kogelbauer et al. (2013) providing continuous and georeferenced vertical profiles by in situ measurements. The system combined two commonly applied soil physical sensors, a capacitive sensor and a penetrometer, synchronized with a GNSS RTK positioning. It enabled the layer delineation of water-mud-cohesive sediment due to the striking differences in the interface characteristics, in contrast to other methods that do not show such distinct transition at the interfaces in their mostly discontinuous profiles. The method was cross-validated by the comparison with echo-sounding data (Heine et al., 2013, 2014) and by ground-truth information from shallow cores. The CSPS was successfully applied in the shallow Neusiedler See.

The Neusiedler See is the largest lake of Austria (315 km^2), and composes of two different ecotopes – the open water and the reed belt (178 km^2) (Dokulil and Herzig, 2009). This endorheic lake is well-mixed and rich in fine-grained sediments that form a distinct mud layer. Owing to its shallowness and wind exposure, the open water zone is characterized by a high concentration of fine-grained suspended sediments (Dokulil and Herzig, 2009). In contrast, the water is completely clear in the reed belt of predominantly *Phragmites* and the open water patches within the reed, but contains a high amount of humus coloides that leads to a yellow to brownish water colour. The inorganic turbidity in the reed is completely missing for two reasons: first the extremely calm water due to less wind exposure and secondly the chemo-physical effects between the humic colloids and the finest-grained sediments. Besides, stormy conditions at the open water only have secondary impact on the turbidity within the reed belt due to water drift from and into the open water (Tauber, 1959).

The reed belt is for the most part an inhomogeneous patchwork of reed, open water areas, and other plants. Thus the reed was differentiated in five main classes with subtypes by age, density, amount of open water areas as well as the amount of other plants (Schmidt and Csaplovics, 2010). The open water patches within the reed are

HESSD
11, 12627–12657, 2014

either classified as considerably sparse old to very old or dying reed with an open water area > 50 % within the reed (class IV and V) or as open water patches with brownish water colour *("Braunwasser")*. In the following these open water areas are labelled as "sparse reed patches" and *"Braunwasser"*. In contrast to that, the inner reed belt and the reed along the lake- and terrestrial borders are assigned to class III, which is defined as sparse to old closed reed with maximal 30 % open water (Schmidt and Csaplovics, 2010). Hence, characteristic layer compositions of water-mud-consolidated lakebed-sediment within these different ecotopes are expected.

The designed CSPS was applied at the different lake's ecotopes: (1) the open water area for referencing echo sounding (Heine et al., 2013, 2014), (2) the shallow water areas below 0.5 m to describe the shore line topography, and where echo sounding is not working (3) the sparse reed patches and the open water patches of brownish colour (*"Braunwasser"*) within the reed, and (4) within the reed. The evidence suggests that the CSPS represents a useful complementary tool that bridges the gap between land- and hydrographic surveying methods.

The objective of this paper is to characterise the layer composition of the different ecotopes obtained from the CSPS profiles. Additionally, some relevant parameters (electrical conductivity and particle size) and wind as affecting external factor are discussed.

2 Methods

2.1 Combination of soil physical sensors in a measuring system (CSPS) and its performance in the field

The combination of soil physical sensors in a measuring system (CSPS) was designed for the sediment layer delineation at shallow lakes, described in Kogelbauer et al. (2013) (Fig. 1, left). It combines two commonly applied soil physical sensors: a capacitive sensor for indirect water content measurements and a modified cone

HESSD
11, 12627–12657, 2014

penetrometer for penetration resistance measurements. The capacitive sensor, the Hydra Probe (Stevens Water Monitoring System) is based on frequency domain reflectometry (FDR) at 50 MHz and measures the dielectric permittivity ε_r to indirectly indicate the volumetric water content θ. The modified cone penetrometer (Eijkelkamp) measures the penetration resistance. Both sensors were combined with a GNSS RTK positioning (Global Navigation Satellite System with Real-time Kinematic) for dynamic, vertical profile-measurements with precise location information (x, y, z) of ±3–5 cm in the overall accuracy. The GNSS antenna was mounted on top of both sensors.

The measurement procedure of the CSPS was similarly conducted at all sites: the open water area, the shallow water areas below 0.5 m, the open water patches within the reed, and within the reed itself (Fig. 1, mid and right panels). The sensors were consecutively used at the same site to create an instantaneously vertical profile in water, mud and consolidated lakebed sediments. The Hydra Probe (HP) measurement started with the sensor head and its tines still in the air. After a few seconds the sensor was slowly inserted in the water and continuously submerged until the compacted mud prevented further penetration of the sensor.

The cone penetrometer (CP) measurement started in the layer where minimal pressure resistance was detected. The sensor was slowly submerged until the consolidated lakebed and deeper when a maximum resistance was reached. The layers of compacted mud and the consolidated lakebed sediments were indicated by a rapidly increasing penetration resistance.

Each sensor measurement was repeated at least three times for the same area to consider local variability of the mud layer structure and the lake bottom topography. At the open water surface the measurements were taken at predefined echo sounding reference points, using a small boat tied up by stakes. At the shoreline, the measurements were taken along a short transect, starting with a point in the reed, going on at the transition from the reed to the open water surface, and finally measuring at the open water. This enabled a description of the lake bed topography at the transition from reed to the open water. The shoreline at the open water patches within the reed was

HESSD
11, 12627–12657, 2014

I. Kogelbauer and W. Loiskandl

similarly investigated with additional points randomly placed at the open water area of these patches. Apart from the investigations by boat at the open water and open water patches, within the reed belt of sparse to closed old reed (class III), according to Schmidt et al. (2010), the measurements were performed from a modified reed cutting machine along transects from the land along the reed to the lake.

2.2 Core sampling and analysis

Sedimentological data were derived from shallow manual coring using a hand core sampler with polycarbonate core tubes. In total 78 cores were collected together with the measured CSPS-profiles. These cores were qualitatively described (colour, consistency and roots) and thus divided into samples of same qualities. These following 141 sediment samples were quantitatively analysed (particle size distribution, total and inorganic carbon, total nitrogen, pH, electrical conductivity, particle density, mineralogy). Two water samples from the open water and 57 water samples from the reed belt were analysed for their pH and electrical conductivity. The aim was to calibrate the HP and to pinpoint the sedimentary succession.

The grain size analysis was made according to the ÖNORM L 1061-1 (Austrian Standards, 2002b) and L 1061-2 (Austrian Standards, 2002a) to determine the predominant fine-sediment grain size classes (Sand (S) from 2 to 0.063 mm, silt (U) from 0.063 to 0.002 mm, and clay (C) below 0.002 mm). The sand fraction was removed by wet sieving and the mass fraction of silt and clay was separated by the pipette method after Kubiena. The texture was classified according to ÖNORM L 1050. Before the chemical analysis, the sediment samples were oven dried (105° C) and sieved (2 mm sieve). Some methods required a filtrate of a sediment suspension. The sediment suspension was made of sediment and distilled water, well-shaked and finally filtrated. The pH value of the sediment samples was measured according to the Austrian Standard ÖNORM L 1083 (Austrian Standards, 2005), whereas in the water samples it was measured immediately without further preparation requirements. The electrical conductivity

HESSD
11, 12627–12657, 2014

was measured in the filtrate of the sediment samples, whereas it was directly measured in the water samples.

2.3 Data acquisition software and analysis

Data from the sensors and the GNSS RTK was collected and processed with a data acquisition system. The main part of the data acquisition system is the therefore developed software tool (GeneCon) based on C# as a console application, see also Kogelbauer et al. (2013). The software (GenePost) was also programmed in C# as a windows forms application and consists of two parts. The first part, the conversion tool, is responsible for raw data conversion incorporating the date format standardization, the calibration functions of the sensors, and the GNSS-Transformation to UTM N 33/WGS 84. The second part, the utilization tool, manages the smoothing function of the penetrometer measurements, the layer detection and combining for a digital elevation model (DEM), and some additional graphical features assisting the graphical data validation.

The calibration functions of the sensors – the Hydra Probe HP (D'Amboise, 2012) and the cone penetrometer CP (Kogelbauer et al., 2013) – were embedded in the conversion tool. The implemented penetration resistance PR function (MPa) was improved in the software, and considered the actual weight of the variable probing rod length Rp, x, which resulted in a varying offset for the force cell for each measurement. The base offset voltage (mV) slightly changed during the operation period; therefore it was set to constant value of 11 mV which was the average during operation in 2013.

For the layer detection in GenePost the raw data of the CP measurements were smoothed to limit the large negative value-peaks of minimal height and to smooth the height loops. First, the large negative values were limited to zero occurring e.g. while shortly pulling on the rods. Secondly, the measurements were sorted according to their height to get a monotone decreasing function of the height and to eliminate the loops. Those loops with small height appeared due to the dynamic reaction (fast moves) of the GPS during the measurement. Finally, the actual smoothing was undertaken; therefore

HESSD
11, 12627–12657, 2014

the maximum penetration resistance PR within each interval of 2 cm height was selected. The height diversion started once from the topmost and once from the bottommost point to include all points also the last lowest maximum penetration resistance. An interval height of 2 cm, according to the maximum GNSS accuracy, was considered the best; a bigger interval reduced the back jumps and the freak values but also considerably reduced the number of data points. The HP raw data were not smoothed at all and taken as they were.

3 Results and discussion

The characteristic layer compositions are presented for the different ecotopes at the shallow, endorheic Neusiedler See: (1) the open water area, see Heine et al. (2014), (2) the open water patches within the reed – sparse reed patches and *Braunwasser*, and (3) the reed.

The influence of external factors – such as chemical parameters, wind, electrical conductivity, and particle size – are discussed sequentially as occurring from top to bottom in the accompanying layer.

The characteristics and important features are highlighted in a representative CSPS profile, illustrated in Fig. 2. It contains the volumetric water content θ ($m^3\,m^{-3}$) (top blue scale), which is indirectly indicated by the HP due to site specific calibration considering different mud layer composition across the lake. This eminent parameter marks the difference between water and mud very precisely. Moreover, it reveals side information on other aspects such as the inorganic turbidity, the electrical conductivity and the sand fraction. The water content reading for the lake water is always lower than 1 because of the inorganic turbidity, especially in the open water, and the variable ecotope-specific electrical conductivity. The HP calibration was done for the mud layer to compensate for varying mud layer composition throughout the lake, and not for the lake water itself.

The HP sensor measurement starts in air and indicates the air–water interface by an increase in θ from zero (air) to about 0.94 (lake water), which is only used as ancillary information. After the sensor submersion in water at an almost constant volumetric water content value θ_{Water}, a striking decrease in θ to considerably smaller values indicates the water–mud interface, equivalent to a lutocline (see Fig. 2). The lutocline is defined as a high density gradient at the interface between clear water on top and the mud suspension underneath (Wolanski et al., 1989). It can occur in turbid environments rich in fine-grained sediments, marine as well as freshwater. It is manifested in a sharp step structure in the vertical profiles of the suspended sediment concentrations or density, which is also present even in the absence of the vertical gradients of temperature and salinity (McAnally et al., 2007; Metha and McAnally, 2008; Schettini et al., 2010; Wolanski et al., 1989).

After the water–mud interface detection, the ongoing HP submersion in the mud suspension might highlight the stratification within the layer and finally stops when the mechanical resistance prevents further penetration of the sensor. Later, the water content at the HP submersion end θ_{HPend} is correlated to the sand fraction of the core samples. Almost concurrently the penetrometer starts registering the incipient penetration resistance $\mathrm{PR_x}$ until the first significant peak $\mathrm{PR_{1st\ peak}}$, which is then accompanied by an abrupt change in slope. This first peak $\mathrm{PR_{1st\ peak}}$ is stated to indicate already fully consolidated lakebed sediment, i.e. the lake bottom. Apparently, this is the interface of a suspension at top, where no effective stress is measured, and the underlying consolidated bed sediment with already measurable effective stress (Metha and McAnally, 2008). Occasionally, a rather distinctive intermediate partially-consolidated layer may occur between the penetration resistance $\mathrm{PR_{0.2}}$ and the first peak $\mathrm{PR_{1st\ peak}}$, depending on the location. The penetrometer detects a consolidated lakebed sediment layer by a constant slope of the penetration resistance due to the equal friction within that layer of same properties. In contrast to that, a peak accompanied by a change in the gradient indicates a change of the sediment properties and hence indicates another sediment layer. The sediment sample layers from coring and the layer delineation are shown next to the CSPS profile. The sediment samples were qualitatively separated (particle size, consistency and colour) in bottom, intermediate and top layer.

HESSD
11, 12627–12657, 2014

3.1 Wind effect on θ_{water} at the open water due to upward diffusion

Fine sediments are stirred up at wind velocities of less than $10\,\mathrm{km\,h^{-1}}$ and cause permanent inorganic turbidity in the wind exposed open water (Dokulil, 1983). However, a gentle turbidity always remains at the open water even at calm wind conditions due to the immanent suspended finest-grained sediments (Sauerzopf and Tauber, 1959); thus, the measured θ_{water} is always below 1.

During the measurement campaign at the open water surface, which was conducted within nine days in spring 2012 and one day re-measurement in summer 2013, it was recognized that the θ_{water} value was influenced by the wind conditions of a preceding period of a few days. In Fig. 3, HP measurements at point P072, which were conducted on a calm day and a windy day with high turbidity, are compared to show the wind effect. θ_{water} was about 0.94 ± 0.02 at calm wind conditions; it was high when the mud accumulation was low and vice versa. During windy conditions θ_{water} was significantly reduced (< 0.9; 0.7–0.8) by the increasing amount of suspended sediments in water due to upward diffusion from the mud layer. Small regional differences were recognized depending on the amount in finest-grained sediments.

Nonetheless, the absolute height of water–mud interface still remained but the lutocline, i.e. the water content gradient, was less pronounced (Fig. 3). Still, the lutocline was always significant and guaranteed precise layer detection. The finding that the lutocline persists even under significant flow-induced forcing, such as strong wind, coincides with Metha and McAnally (2008). Moreover, the time-independence of measurements within two consecutive years was addressed, since θ was measured in 2012 and θ-Wind was measured in 2013. The measured absolute layer heights from consecutive years remained within the overall system accuracy.

3.2 $\theta_{HP\ end}$ vs. sand fraction at the open water

Another important aspect is that the vol. water content at the HP submersion end $\theta_{HP\ end}$, where the mechanical resistance prevents further ongoing, is subject to the

HESSD
11, 12627–12657, 2014

amount of sand fraction at the corresponding height. The average $\theta_{\text{HP end}}$ was generally lower at the presence of at least 6 % amount of sand fraction in the clay and silt dominated environment (Table 1).

Remarkably, some measurements of low $\theta_{\text{HP end}}$ values at almost no amount of sand fraction in the corresponding core sample showed extremely high electrical conductivity in the lakebed-sediment filtrate (located at Rust).

3.3 Selected chemical parameters and soil texture of the ecotopes

The Neusiedler See can be qualified as a sodium bicarbonate lake, containing now up to $2\,\text{g}\,\text{L}^{-1}$ of salts (Herzig and Dokulil, 2001). Generally, the electrical conductivity is 1300–3200 $\mu\text{S}\,\text{cm}^{-1}$ and a pH value > 8 (Herzig and Dokulil, 2001), but it varies across the ecotopes with completely different environmental conditions.

The chemical analysis of the water samples in the reed area at the western shore showed an average electrical conductivity of 2061 $\mu\text{S}\,\text{cm}^{-1}$ which was significantly higher than the avereage of 727 $\mu\text{S}\,\text{cm}^{-1}$ at the open water (Table 2). The pH of water within the reed was 7.5 and therefore also lower than that of the open water (pH 8.7).

The chemical analysis of the sediment sample filtrates showed the highest electrical conductivity for those from the reed and the highest pH for samples from the *Braunwasser*, which were located south-east in the national park area (Table 2). The total carbon C_{tot}, total nitrogen N_{tot}, and the electrical conductivity were higher in the reed than at the open water area (unpublished results); whereas pH was almost similar. The soil texture triangle gained from particle size analysis of all samples (without height separation – bottom, intermediate, and top layer) highlighted a highly clay (C) dominated environment at the open water, a loamy Clay (lC) to silty Loam (sL) environment at the spares reed patches in the north-west surrounding the Wulka River mouth, and a loamy Clay (lC) to clayey Sand (cS) environment in the *Braunwasser* in the south-east (Fig. 4).

HESSD
11, 12627–12657, 2014

3.4 HP–CP overlap of the vertical measurement range from the Hydra Probe and the cone penetrometer

The HP-CP overlap depicts the height difference ranging from the HP submersion end to the first significant penetration resistance signal $PR_{0.2}$ at 0.2 MPa for the nearest neighbouring measurement of each sensor (Fig. 2). The maximum distance to the nearest measurement neighbour is set to 0.5 m. This HP-CP overlap for the open water area was in average −0.02 m (Standard Deviation SD 0.19), so the penetrometer's first detection signal lies above the last HP signal. Hence, a continuous vertical profile was supported by the combination of those two sensors. In the reed the average overlap of about −0.09 m (SD 0.30) was even bigger than at the open water area. This is explained due to an early but small penetration signal, while pushing through the top rhizome layer (see also Fig. 6e). These early signals fad quickly and soon increase to significant values of penetration resistance of the lake bottom.

3.5 Consolidated lakebed – knick point in penetration resistance

According to Metha and McAnally (2008), the bed can be differentiated from the mud suspension above by the measureable effective normal stress. The measureable stress is partially nil above the lakebed surface and increases below it with increasing concentration or density. Above the fully consolidated bed showing already considerable effective stress, a newly deposited or partially consolidated layer show gradually increasing effective stress and may still undergo deformations (Metha and McAnally, 2008; Whitehouse et al., 2000).

Thus, the consolidated lakebed is defined as the first significant peak or knick point in the penetration resistance $PR_{1st\ peak}$ higher than 0.8 MPa frequently together with an abrupt change of slope i.e. less increase in PR with increasing penetration depth. The knick point in penetration resistance is typically due to a change in friction that indicates changing sediment properties.

HESSD
11, 12627–12657, 2014

I. Kogelbauer and W. Loiskandl

The above partially consolidated layer ranges from the signal $PR_{0.2}$ at 0.2 MPa (discussed in Sect. 3.4), to the defined $PR_{1st\ peak}$ signal at 0.8 MPa. The height of the partially consolidated layer at the open water area was in average 0.24 m (SD 0.23) and may reach up to 1.34 m in maximum. It is considered to be the incipient state of consolidation formed either due to settling or due to an evolving pore structure where the cone penetration force is already diverted (Whitehouse et al., 2000). Thus, this intermediate layer is on the point of losing the characteristics of a water-driven mud suspension at the open water.

The shape of the penetration function is affected by numerous factors, such as the particle size distribution, the wind-induced current, the organic content, the sediment mineralogy, and the consolidation and coagulation processes. However about four main penetration signal types A to D are predominantly found. The signal types A to B mainly occur at the open water area, the signal type C occurs at the open water patches within the reed, and signal type D predominantly occurs in the reed (Fig. 5).

At the open water area, the penetration type correlates to the particle size distribution. Type A shows a consolidated lakebed at the knick point of penetration resistance $PR_{1st\ peak}$ at about 0.8 MPa and above a partially consolidated layer of intermediate resistance. This type mainly occurs at distinct mud layer and no or small amount of sand fraction. In other words, if the clay fraction is > 50 % mass, the knick point $PR_{1st\ peak}$ occurs at about 0.8 MPa at a steep slope i.e. less increasing PR at a high increase in penetration depth ($\Delta PR \ll \Delta h$). If the silt content equals the clay content or the sand fraction is higher than 3 %, the $PR_{1st\ peak}$ is at about 1 MPa, which displays Type B (Fig. 5). In this case, the slope is flat and PR rapidly increases at small penetration depth ($\Delta PR \gg \Delta h$). The discrepancy of the height difference from the existing peak at about 1.0 MPa to the defined lake bottom at 0.8 MPa is negligible. Reason is the flat slope and the therefore marginal height difference. This thin, highly compacted lakebed layer prevents further penetration due to a high degree of compaction, which agrees with the echo sounding results showing strong and clear reflection (Heine et al., 2014).

HESSD
11, 12627–12657, 2014

Type C occurs at the less wind exposed open water patches – sparse reed patches and *Braunwasser* – within the reed. The consolidated lake bed is clearly defined by the $PR_{1st\,peak}$ with an abrupt change in slope. Small subsurface strata of weak PR occur. Type D is predominant in the reed with the characteristic small incipient PR caused by penetrating the top rhizome layer. The penetration resistance increases progressively with deep penetration. This is followed by a rapid increase from 0.8 to 1.5 MPa or even higher accompanied by a slope change that indicates the $PR_{1st\,peak}$. The deepest penetration depth is reached in the reed.

3.6 Ecotope-specific characteristics of the CSPS profiles

Finally, the ecotope-specific CSPS profiles (overview in Fig. 1, right panel) are shown and discussed concerning their characteristics (Fig. 6). According to the reed classification used in Schmidt et al. (2010) the selected ecotope points within the reed are assigned as followed: L355 is assigned to considerable sparse old reed (class IV) already close to the *Braunwasser*, A311 is in a large area of *Braunwasser*, and L606 is assigned to sparse old reed (class III).

At the open water area, the inorganic turbidity of the suspended sediment load in water is immanent and increases with wind. This corresponds with the measured θ_{Water} at the open water which remained always below 1 (Fig. 6a and b). At the open water a distinct lutocline allows a precise delineation of the water–mud interface because of a gradient in water content > 10 % from θ_{Water} to θ_{LC} (Table 3, Fig. 6a and b). The water content at the submersion end θ_{HPend} is affected by the particle size distribution (see Sect. 3.2). The extent between $PR_{0.2}$ and $PR_{1st\,peak}$ suggests the presence of a partially consolidated layer that may undergo deformations and depends on the wind exposition and the potential of sediment accumulation. Likewise, the penetration resistance function as well as the resistance peak $PR_{1st\,peak}$ at the open water depends on the predominant current, the predominant particle size distribution, the organic content as well as the mineralogical composition. The comparison of two open water sites displays some perceptible trends of the penetration resistance: shallow strata within the

HESSD
11, 12627–12657, 2014

shallow subsurface can be observed at strong current exposed areas (Fig. 6a); a high sand and silt content supports a rapid increase in penetration resistance and a higher peak (Fig. 6b), which is also shown in the particle size distribution of the sediment cores (Fig. 7). The CSPS profiles at the open water were used for the purpose of layer validation for the echo sounding data (Heine et al., 2013, 2014). The layer validation considerably coincided in both, the detected water–mud interface and the consolidated lake bed.

At the sparse reed patches θ_{Water} was even higher than at the open water due to the missing inorganic turbidity in the extremely calm water (Table 3), which is also prevailing during stormy conditions (Dokulil and Herzig, 2009; Sauerzopf and Tauber, 1959). Compared to that, θ_{Water} at the *Braunwasser* was about 0.86 and therefore lower. It was also generally lower than at the open water because no wind-induced turbidity persists. But it was also lower than at the sparse reed patches because the high electrical conductivity damped θ_{Water}. At these less wind-exposed areas the settling process is accelerated where a distinct lutocline cannot evolve (Fig. 6c and d). The penetration depth was lower in the middle of the open water patches than at its shore to the reed. The layer between $\text{PR}_{0.2}$ and $\text{PR}_{\text{1st peak}}$ was in average 0.26 (SD 0.24) and suggested to be partially consolidation. Nevertheless, the incipient penetration resistance started already at the HP submersion end and supported a continuous profile. The core samples taken at the *Braunwasser* (located south-east in the national park area) showed higher content in sand fraction than those from the sparse reed patches (north-west surrounding the Wulka River mouth) (Fig. 7).

In the reed areas, the volumetric water content θ_{Water} was in average 0.80 due to damping of the dielectric permittivity ε_{r} by a relatively high electrical conductivity (Table 3). The root system in the reed limits the development of a lutocline, and thus disrupts precise mud layer delineation. However a decreasing trend until $\theta_{\text{HP end}}$ of about 0.70 in average was still given, whereas $\theta_{\text{HP end}}$ at the open water areas declineed to an average of about 0.57. Reasons are the measurements within the reed rhizome with intrinsic high organic content, as well as a shallow submersion end not below the dense rhizome stock. The declining θ indicates an increasing amount of solids and delineates together with the early but low penetration resistance a layer composed of non-consolidated suspended sediments and rhizomes. Hence a mud-rhizome layer is delineated from $PR_{0.2}$ to $PR_{1st\ peak}$. Moreover, the high water content at the submersion end $\theta_{HP\ end}$ also justified the slow but continuous increase of the penetration resistance until $PR_{1st\ peak}$ with an accompanying slope change (Fig. 6e). $PR_{1st\ peak}$ within the reed was mostly about 1.5 to 2 MPa. In the reed, the low degree of consolidation and the material composition supports the maximal possible penetration depth compared to the other ecotopes. The particle size distribution showed generally higher content in sand fraction than at the open water. Layers rich in sand fraction of 10 up to 60 % were occasionally detected in the core samples as well during the penetration.

4 Conclusion

Although many studies report the exploration of the sedimentary structure in marine or lake environments, a reliable method for investigating the sediment layer composition of the same sediment body from the transition of land to water is still missing. The previously introduced combination of soil physical sensors in a measuring system (CSPS) provided a rapid in situ technique for the delineation of the water-mud-consolidated lakebed interfaces at different ecotopes at a shallow lake rich in fine-grained sediments. The CSPS, was successfully applied in the shallow Neusiedler See and provided characteristic layer compositions for the different ecotopes (the open water, the open water patches within the reed, and the reed).

The Hydra Probe, a well-known sensor, represents a new and highly valuable device for the layer delineation of the water–mud interface at the open water due to a pronounced lutocline. The lutocline may be damped by factors such as a high electrical conductivity or wind-induced turbidity, but still supports precise water–mud interface delineation at the open water and the open water patches. In the reed the root system

HESSD
11, 12627–12657, 2014

limits the development of a lutocline and thus, disrupts precise mud layer delineation with the Hydra Probe.

The cone penetrometer is already well known for detecting shallow sub-bottom strata at the open water. It was also successfully applied in the different lake environments. The delineation of the consolidated lakebed within the ecotopes is performed with the same principles but show ecotope-specific characteristics. At the open water either a shallow and highly compacted consolidated lakebed or a consolidated lake bed with a partially compacted layer above (detected in bays located at Rust in the south-west and at some places in the north) was observed. The occurrence depends on the mud accumulation potential (predominant current, finest-grained sediment supply, wind exposure, etc.). In the reed, the penetration resistance smoothly increases reaching the deepest penetration depths compared to the other ecotopes. The distinct layer between $PR_{0.2}$ and $PR_{1st\ peak}$ in the reed suggests a composition of less consolidated mud and rhizome. In comparison, at the open water areas and open water patches this layer suggests partially consolidated sediments.

Overall, the study indicates that the CSPS is a powerful tool for screening shallow lake environments. The CSPS represents moreover a useful complementary tool that bridges the gap between land- and hydrographic-surveying methods.

This study represents an indispensable requirement for ecosystem characterization and contributes to establish a digital elevation model (DEM) of the mud layer and the lake bed, as part of the project "Geodetic survey of the system Neusieder See – Hanság Channel". Nonetheless it has a stand-alone value that underlines the characteristic composition of various lake ecotopes.

This integrative approach of lake ecotope characterization supports management and ecosystem services to find a trade-off with competing human uses. The CSPS approach is applicable in a wide range of wetlands and lake environments to characterize sediment layer compositions.

HESSD
11, 12627–12657, 2014

Author contributions. I. Kogelbauer designed the study, designed the method, performed research, analysed data, and wrote the paper with substantial input and edits from W. Loiskandl. W. Loiskandl conceived the study, contributed new methods, and supervised the research.

Acknowledgements. We thank Wolfgang Sokol for the technical support and software design and Erwin Heine for the support in the GNSS application. Thanks also to the measurement crew and the Biologische Station Illmitz for their technical support and facility provision. Funding for field work was granted by the European Regional Development Fund (ERDF) Cross border Cooperation Program Austria – Hungary 2007–2013 (Acronym: "GeNeSee"; Project Nr: ATMOS/L00130).

References

Austrian Standards: Physical Analysis of Soils – Determination of Particle Size Distribution in Mineral Soils – Part 2: Fine Soil (ÖNORM L 1061-2), Vienna, 2002a.

Austrian Standards: Soils From Waste – Part 1: Fractional Analysis – Methods of Analysis (ÖNORM L 1061 1), Vienna, 2002b.

Austrian Standards: Chemical Analyses of Soils – Determination of Acidity (pH Value) (ÖNORM L 1083), Vienna, 2005.

Dokulil, M.: Assessment of components controlling phytoplankton photosynthesis and bacterioplankton production in a shallow, alkaline, turbid lake (Neusiedlersee, Austria), Univeristät Wien, Wien, Austria, 1983.

Dokulil, M. T. and Herzig, A.: An analysis of long-term winter data on phytoplankton and zooplankton in Neusiedler See, a shallow temperate lake, Austria, Aquat. Ecol., 43, 715–725, doi:10.1007/s10452-009-9282-3, 2009.

Heine, E., Prokoph, A., Kogelbauer, I., and Loiskandl, W.: Hydroakustische Erfassung der Morphologie und Sedimentschichtung des Neusiedler Sees, in: 17. Internationale Geodätische Woche Obergurgl 2013, edited by: Hanke, K. and Weinold, T., Herbert Wichmann Verlag, Obergurgl, AT, 64–75, 2013.

Heine, E., Kogelbauer, I., Prokoph, A., and Loiskandl, W.: Hydrographical surveying of the steppe lake Neusiedler See – Mapping the lake bed topography and the mud layer, J. Photogramm. Remote Sens. Geoinf. Sci., 5, 339–350, 2014.

Herzig, A. and Dokulil, M.: Neusiedler See – ein Steppensee in Europa, in: Ökologie und Schutz von Seen, edited by: Dokulil, M., Hamm, A., and Kohl, J.-G., Facultas UTB, Vienna, 401–415, 2001.

Kogelbauer, I., Heine, E., D'Amboise, C., Müllebner, C., Sokol, W., and Loiskandl, W.: Adaptation of soil physical measurement techniques for the delineation of mud and lakebed sediments at Neusiedler See, Sensors , 13, 17067–17083, doi:10.3390/s131217067, 2013.

Lambert, D. N., Kalcic, M. T., and Faas, R. W.: Variability in the acoustic response of shallow-water marine sediments determined by normal-incident 30 kHz and 50 kHz sound, Mar. Geol., 182, 179–208, doi:10.1016/S0025-3227(01)00234-1, 2002.

McAnally, W. H., Teeter, A., Schoellhamer, D., Friedrichs, C., Hamilton, D., Hayter, E., Shrestha, P., Rodriguez, H., Sheremet, A., Kirby, R., and Fl, A. T. C. M.: Management of fluid mud in estuaries, bays, and lakes, II: Measurement, modeling, and management, J. Hydraul. Eng., 133, 23–38, doi:10.1061/(ASCE)0733-9429(2007)133:1(23), 2007.

Metha, A. J. and McAnally, W. H.: Fine-grained sediment transport, in: Sedimentation Engineering: Processes, Measurements, Modeling and Practice, edited by: Marcelo, H. G., American Society of Civil Engineers, New York, 1132 pp., 2008.

Missiaen, T., Slob, E., and Donselaar, M. E.: Comparing Different Shallow Geophysical Methods in a Tidal Estuary, Verdronken Land van Saeftinge, Western Scheldt, the Netherlands, 151–164, 2008.

Sauerzopf, A. and Tauber, A. F. (Eds.): Landschaft Neusiedlersee, Grundriss der Naturgeschichte des Großraumes Neusiedlersee, Burgenländisches Landesmuseum (Amt der Bgld. Landesregierung, Abteilung XII/1-LM), Eisenstadt AT, 1959.

Schettini, C. A. F. Ç., Almeida, D. C., Siegle, E., and Alencar, A. Ô. C. B. Ã.: A snapshot of suspended sediment and fluid mud occurrence in a mixed-energy embayment, Tijucas Bay, Brazil, Geo-Mar. Lett., 30, 47–62, doi:10.1007/s00367-009-0152-8, 2010.

Schmidt, J. and Csaplovics, E.: Mapping the Austrian reed bed of Lake Neusiedl by means of airborne optical scanner imagery, in: International Symposium on Advanced Methods of Monitoring Reed Habitats in Europe, Illmitz, AT, 2010.

Schrottke, K., Becker, M., Bartholomä, A., Flemming, B. W., and Hebbeln, D.: Fluid mud dynamics in the Weser estuary turbidity zone tracked by high-resolution side-scan sonar and parametric sub-bottom profiler, Geo-Mar. Lett., 26, 185–198, doi:10.1007/s00367-006-0027-1, 2006.

HESSD

11, 12627–12657, 2014

Characterization of sediment layer composition in a shallow lake

I. Kogelbauer and W. Loiskandl

Seifert, A. and Kopf, A.: Modified dynamic CPTU penetrometer for fluid mud detection, J. Geotech. Geoenviron. Eng., 138, 203–206, doi:10.1061/(ASCE)GT.1943-5606.0000563, 2012.

Seifert, A., Stegmann, S., Mörz, T., Lange, M., Wever, T., and Kopf, A.: In situ pore-pressure evolution during dynamic CPT measurements in soft sediments of the western Baltic Sea, Geo-Mar. Lett., 28, 213–227, doi:10.1007/s00367-008-0102-x, 2008.

Shi, Z., Ren, L. F., and Lin, H. L.: Vertical suspension profile in the Changjiang Estuary, Mar. Geol., 130, 29–37, doi:10.1016/0025-3227(95)01396-2, 1996.

Soja, A.-M. and Soja, G.: Deliverable 3.1.2, Colonisation History by Harmful Algue; Lake Neusiedl (Project EULAKES Ref. Nr. 2 CE243P3), Tulln, Austria, available at: http://www.eulakes.eu/upload/eulakes/gestionedocumentale/3.1.220final20N_784_2662.pdf, last access: 25 September 2014.

Tauber, A. F.: Trübung und Sedimentverfrachtung im Neusiedlersee, in: Landschaft Neusiedlersee, Grundriss der Naturgeschichte des Großraumes Neusiedlersee, edited by: Sauerzopf, A. and Tauber, A. F., Burgenländisches Landesmuseum (Amt der Bgld. Landesregierung, Abteilung XII/1-LM), Eisenstadt, AT, 81–88, 1959.

Teeter, A. M.: The viscous characteristics of channel-bottom muds, Technical Note DRP-2-04, US Army Engineer Waterways Experiment Station, Vicksburg, MS, 1992.

Tolotti, M.: Transnational Output 3.1.4, Final transnational report on long term ecological evaluation of CE lakes (Project EuLakes Ref. Nr. 2 CE243P3), Istituto agrario di San Michele all'Adige, Fondazione Edmund Mach di San Michele all'Adige, San Michele All'adige, Italy, 2012.

Whitehouse, R., Soulsby, R., Roberts, W., and Mitchener, H.: Dynamics of Estuarine Muds: a Manual for Practical Applications, Thomas Telford, Wallingford, England, UK, 2000.

Wolanski, E., Asaeda, T., and Imberger, J.: Mixing across a lutocline, Limnol. Oceanogr., 34, 931–938, 1989.

HESSD
11, 12627–12657, 2014

I. Kogelbauer and W. Loiskandl

Table 1. $\theta_{HP\ end}$ related to the amount of sand fraction at the open water.

	p[S] (%)	p[U] (%)	p[C] (%)	θ_{Water} ($m^3\ m^{-3}$)	$\theta_{HP\ end}$ ($m^3\ m^{-3}$)
Sand fraction S > 6 %	39.73 (27.65)	22.80 (9.32)	37.48 (18.88)	0.95 (0.01)	0.54 (0.03)
Sand fraction S < 6 %	2.38 (1.41)	39.08 (7.32)	58.54 (7.79)	0.90 (0.07)	0.58 (0.05)

Without measurements of two extraordinary sites of high electrical Conductivity or sand fraction > 90 % (located at Rust and Vogelinsel, respectively).
Average value and below SD in parenthesis.
Sediment grain size classes: sand (S) from 2 to 0.063 mm, silt (U) from 0.063 to 0.002 mm, and clay (C) below 0.002 mm.

HESSD
11, 12627–12657, 2014

Table 2. Chemical parameters (pH, electrical conductivity) for all sediment and water samples.

Average	pH	Electrical Conductivity ($\mu S\,cm^{-1}$)	N
Sediment samples			
Open water	8.6 (0.2)	725 (230)	81
Sparse reed patches	8.1 (0.3)	812 (602)	18
Braunwasser	9.1 (0.3)	591 (304)	16
Reed	8.4 (0.3)	1003 (303)	18
Water samples			
Open water	8.7 (0.0)	727 (8)	2
Reed	7.5 (0.3)	2061 (901)	57

Average value of ecotope-specific samples (without height separation); SD in parenthesis; N = sample size.

HESSD
11, 12627–12657, 2014

Table 3. Ecotope-specific vol. water content for water θ_{Water}, at the lutocline θ_{LC}, and at the HP submersion end θ_{HPend}.

	Open water	Sparse reed patches	Braunwasser	Reed
θ_{Water} ($m^3\,m^{-3}$)	**0.87** (0.11)	**0.91** (0.07)	**0.81** (0.10)	**0.80** (0.12)
θ_{LC} ($m^3\,m^{-3}$)	**0.76** (0.09)	**0.80** (0.06)	**0.71** (0.09)	**–[*]** –[*]
θ_{HPend} ($m^3\,m^{-3}$)	**0.57** (0.09)	**0.67** (0.09)	**0.57** (0.11)	**0.70** (0.09)

Average value and below SD in brackets.
Sample size N: open water patches (704); sparse reed patches (486); Braunwasser (182); reed (558).
[*] Lutocline is not present.

HESSD
11, 12627–12657, 2014

Characterization of sediment layer composition in a shallow lake

I. Kogelbauer and W. Loiskandl

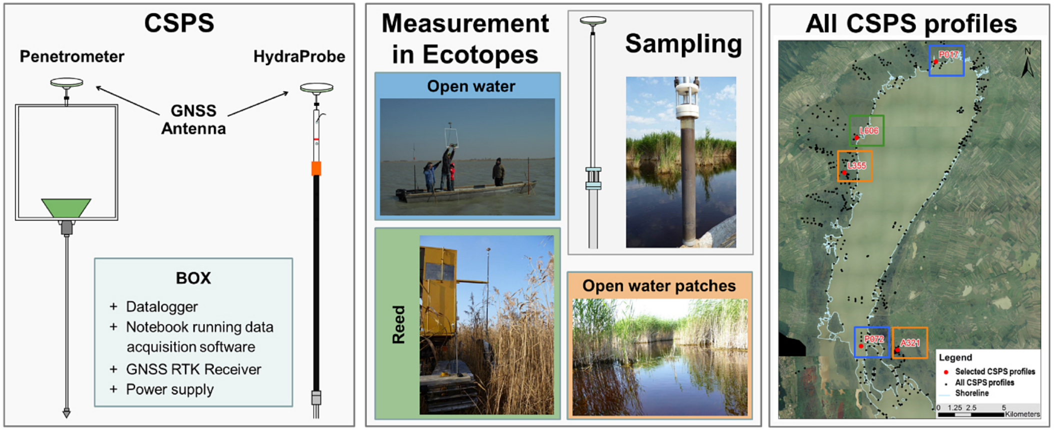

Figure 1. The overview shows the designed system (CSPS), the measurement in the different ecotopes in representative pictures, the sampling equipment, and all measured CSPS profiles at the study site Neusiedler See. The selected ecotope-specific CSPS profiles are highlighted in corresponding colour.

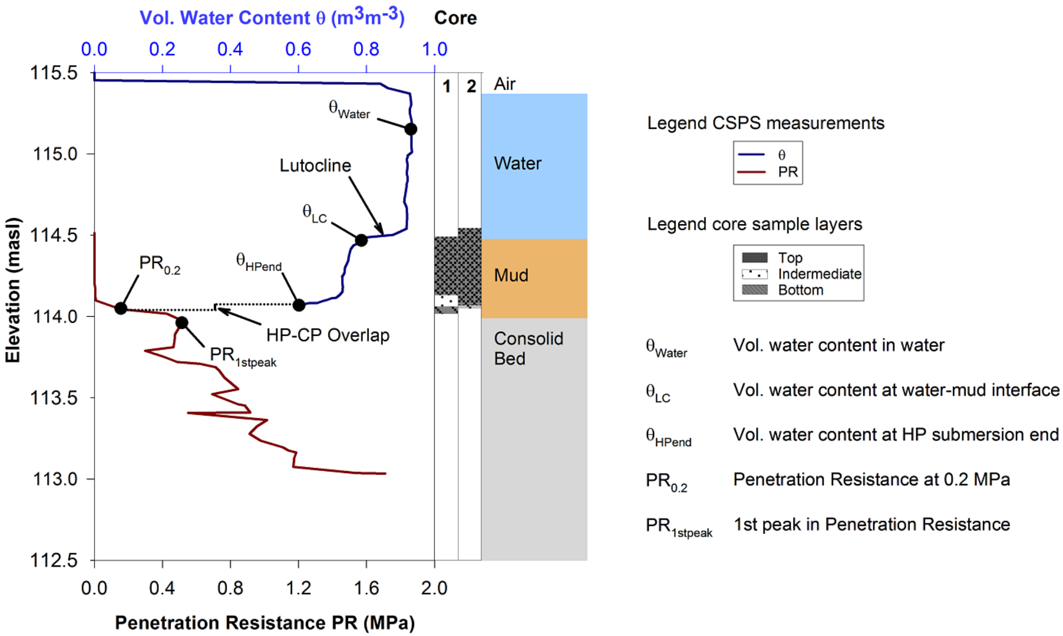

Figure 2. Characteristic features highlighted in a typical CSPS profile.

HESSD
11, 12627–12657, 2014

I. Kogelbauer and W. Loiskandl

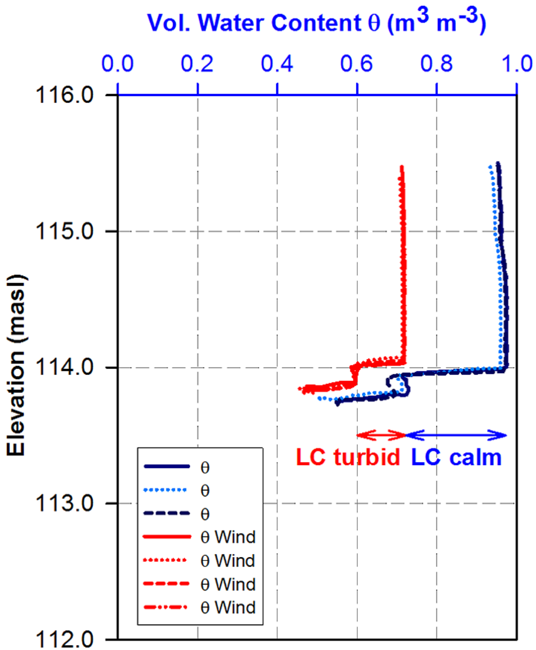

Figure 3. Volumetric water content θ_{water} and the lutocline LC are affected by the wind induced upward diffusion: the lutocline LC, which indicates the water–mud interface, is more pronounced during calm conditions (θ, LC calm, blue) rather than during windy conditions (θ-Wind, LC turbid, red). The absolute height of the interface is not wind affected. A good repetition of several consecutive measurements is shown too.

HESSD
11, 12627–12657, 2014

Characterization of sediment layer composition in a shallow lake

I. Kogelbauer and W. Loiskandl

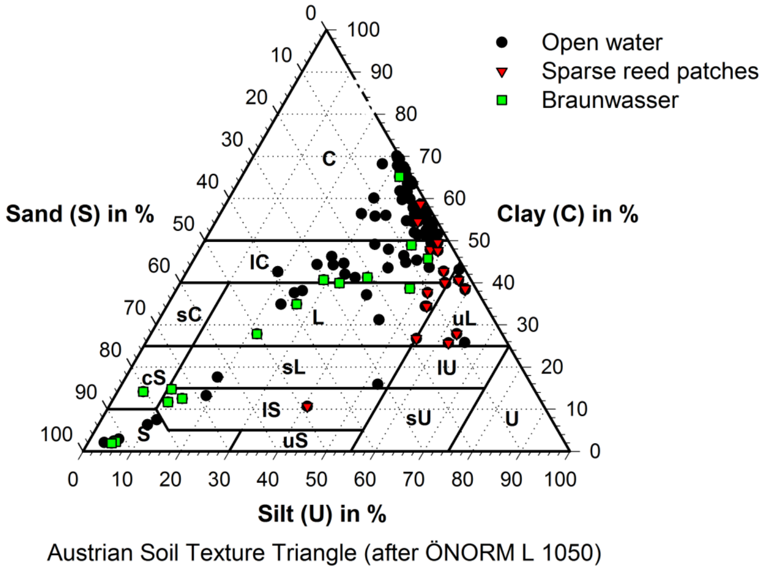

Figure 4. Soil Texture Triangle (after ÖNORM L 1050) including all ecotope-specific sediment samples. It highlights a highly clay dominated environment, especially at the open water. A trend to clay content below 50 % is evident for the water patches within the reed.

HESSD
11, 12627–12657, 2014

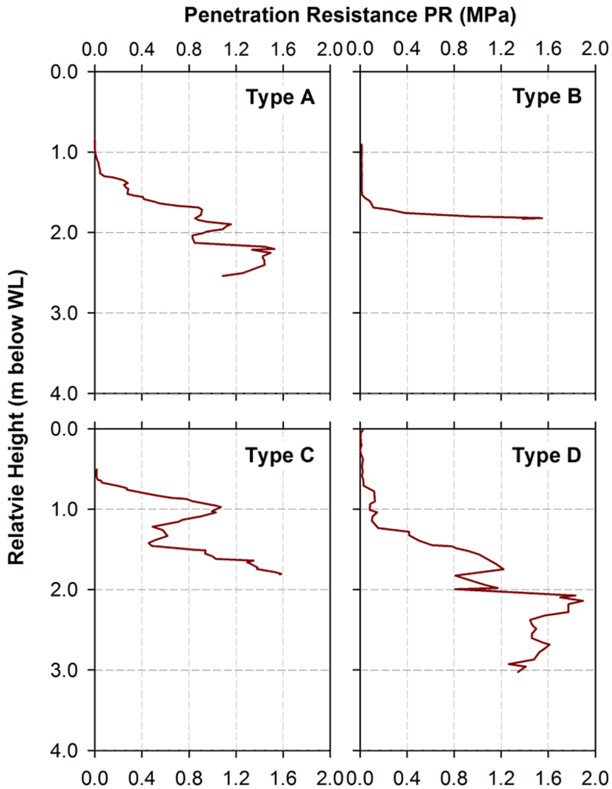

Figure 5. Compilation of the main penetration signal types. They are shown relative to the prevailing water level WL at the actual measurement.

HESSD
11, 12627–12657, 2014

Characterization of sediment layer composition in a shallow lake

I. Kogelbauer and W. Loiskandl

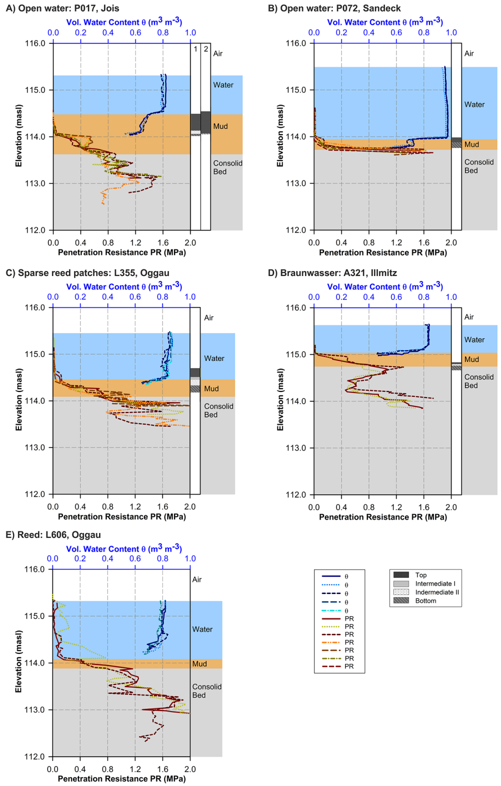

Figure 6. Representative ecotope-specific CSPS profiles for the in situ layer delineation are shown for the open water (**a** and **b**), sparse reed patches **(c)**, Braunwasser **(d)**, and for the reed **(e)**. The HP measurement of the volumetric water content θ ($m^3\,m^{-3}$) delineates the water–mud interface by its sudden decline. The mud-bed sediment interface is detected by the penetration resistance $PR_{1st\ peak}$ (MPa) at the shallowest significant peak accompanied by an abrupt change of slope. In the reed a lutocline is abscent, but the mud layer composing of less consolidated sediments and rhizomes is delinated from $PR_{0.2}$ to $PR_{1st\ peak}$.

HESSD
11, 12627–12657, 2014

I. Kogelbauer and W. Loiskandl

Title Page
Abstract | Introduction
Conclusions | References
Tables | Figures
◀I | ▶I
◀ | ▶
Back | Close
Full Screen / Esc
Printer-friendly Version
Interactive Discussion

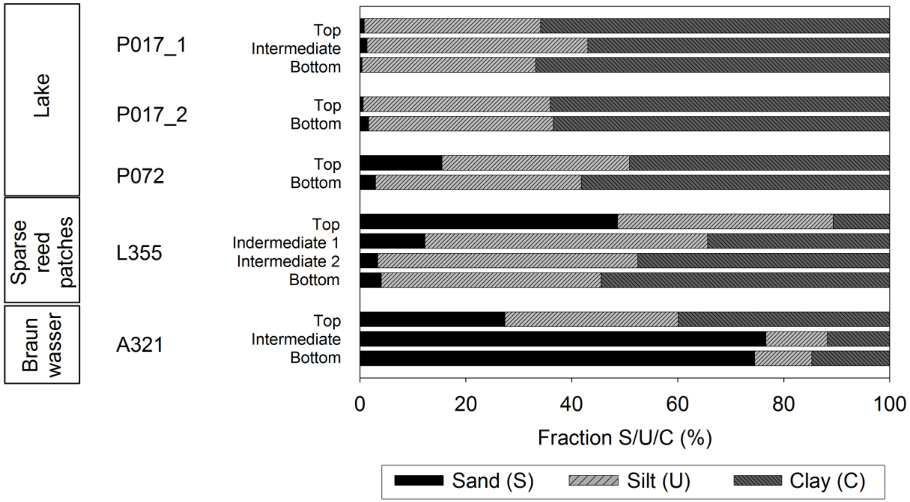

Figure 7. Particle size distribution of the ecotope-specific CSPS profiles in Fig. 6, if coring is available. The two samples at point P017 show a comperalbe distribution.

HESSD
11, 12627–12657, 2014

Characterization of sediment layer composition in a shallow lake

I. Kogelbauer and W. Loiskandl